# Noise Analysis of a Wide-Band Multiuser Fieldbus Communication Scheme with Discrete Multitone

Thomas Handte, and Joachim Speidel
Institute of Telecommunications, University of Stuttgart, Germany
Email: {handte, speidel}@inue.uni-stuttgart.de

***Abstract*—We analyze the signal-to-noise ratio (SNR) of a multiuser fieldbus communication scheme which applies discrete multitone (DMT) modulation. In particular, we derive very accurate analytical expressions on the SNR in down- and uplink. Thereby each subscriber is modeled by a transmit and receive circuit which comprises major noise sources. It turns out that a strong noise funneling arises in uplink where several subscribers have simultaneously access to the channel. For that reason, we derive two low-complexity optimization strategies where one compensates for the near-far effect and the other optimizes the operating point of the digital-to-analog converter. The presented methods provide fairness between subscribers and a significant gain in uplink SNR, simultaneously. Besides, we analyze exemplary networks and show that simulation results are in excellent agreement with our analytical expressions. Additionally, both illustrate that optimization can yield gains of several dBs in uplink SNR such that the fieldbus communication scheme offers comparable SNR performance in both communication directions.**

## I. Introduction

In recent years, the need for higher data rates in industrial fieldbus communication schemes has continuously increased. Especially in low-level applications only a few bits were transmitted between a central data collection unit (master) and various sensors or actuators (slaves) because only rather simple devices had to be served. In future, more intelligent devices will demand a larger amount of data to be transmitted while key parameters imposed by process and factory automation like real-time capability, high quality of service (QOS) and very low bit error rate (BER) need still to be guaranteed. Additionally, communication networks in the industrial field need to be very flexible in the sense that arbitrary number of slaves with arbitrary data rate can be positioned in any user-defined position along a transmission line (multidrop feature). This imposes a challenge for the system since it has to be highly adaptive with respect to changing operating conditions. Due to these obligatory requirements, current low-level fieldbus communication schemes are forced to operate at their performance edge. Their data throughput can only be increased slightly because a higher clock rate of line coded signals would result in strong intersymbol interference. As a result, the BER and the retransmission rate (RTR) of erroneously received messages would rise unacceptably.

Thus, new communication concepts using state-of-the-art digital modulation techniques are essentially required. The concept proposed in [1] features discrete multitone (DMT) [2] which divides the transmission bandwidth into narrow band carriers. They are individually allocated to every slave depending on both the actual position within the network and the desired data rate. The carriers are also used for multiuser separation since the data of each slave is modulated on distinct carriers which are mutually orthogonal to each other. Thus, parallel access is achieved and by applying time-division duplex a bidirectional link is established. For safeguarding the bits to be transmitted, a novel forward error correction was developed in [3] which assures a BER of $10^{-9}$ or even lower while the RTR is kept low, simultaneously.

Further work has been done in [4] and [5] where network management procedures and media access organization have been described. Moreover, in [6] a prototypical circuit for real-time evaluation of the concept has been presented. It was experimentally shown [4] that the scheme can access up to 128 slaves, provides round-trip times as low as 1 ms, and offers a very low BER despite the very harsh industrial field.

In this paper, we focus on the system performance in terms of the achievable SNR which is the crucial parameter for high QOS as well as low BER and RTR [3]. We therefore analyze a very general transmit and receive circuit which comprises noise sources like amplifiers and digital-analog (DAC) as well as analog-digital (ADC) converters. In a next step, we give analytical expressions on the SNR seen by every subscriber in a multiple access scenario for both downlink (DL) and uplink (UL). Based on that, we optimize transmission quality in UL by choosing the transmit amplifications of the slaves such that they compensate for the near-far effect. This is shown to yield an SNR gain and fairness between slaves. Besides, the operating point of the DAC is optimized to the UL scenario where a single slave modulates only a small portion of available carriers. Using these optimization techniques, simulation results show that UL SNR can be tremendously increased and that DL and UL achieve similar SNR performance.

The paper is organized as follows: Section II introduces the system model whereas in Section III we derive an analytical noise model for DL and UL. Optimization of system performance is presented in Section IV and selected analytical and simulation results are shown in V while Section VI concludes the paper.

## II. System Model

We consider a multiuser fieldbus with $N+1$ subscribers namely one master and $N$ slaves where each is modeled by an equivalent circuit shown in Fig. 1. Subscriber $i$ features input impedance $Z$, a transmit as well as a receive circuit. Subscriber $i$ transmits data by modulating current $I_i$ and it evaluates voltage $U_i$ for demodulating data.

978-1-4673-6361-7/13/$31.00 

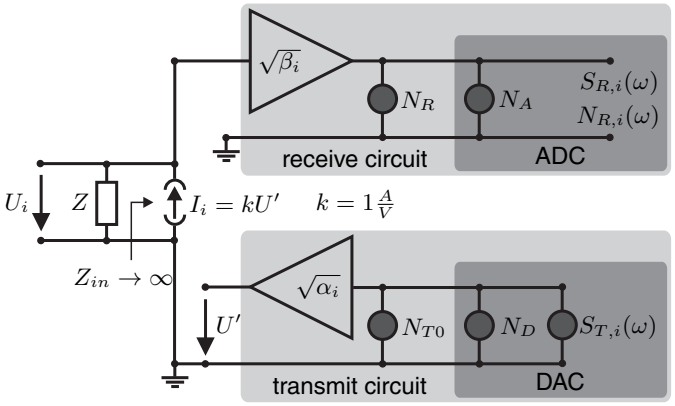


Fig. 1. Equivalent circuit of a subscriber.

In more detail, the transmit circuit consists out of a DAC followed by a noisy transmit amplifier with amplification $\sqrt{\alpha_i}$ which provides the control-voltage for transmit current $I_i$. The DAC generates a DMT signal with power spectrum density (PSD) $S_{T,i}(\omega)$. Clipping and quantization noise are combined in PSD $N_D$ while the amplifier noise is given by PSD $N_{T0}$. Both are assumed to be frequency flat.

On the other hand, the receive circuit features an amplifier with amplification $\sqrt{\beta_i}$ in combination with a noise source with frequency-flat PSD $N_R = \beta_i N_{R0}$. Subsequently, an ADC transforms the amplified received signal with PSD $S_{R,i}(\omega)$ in digital domain where demodulation is performed. Addtionally, the ADC adds noise with the frequency-flat PSD $N_A$.

The subscribers operate within a wireline network with arbitrary topology. For illustration Fig. 2 shows an exemplary setup. The transfer function from the master with current $I_0(\omega)$ to slave $i$ is denoted by

$$H_i(\omega) = \frac{U_i(\omega)}{I_0(\omega)} \quad i = 1, \ldots, N \tag{1}$$

where $H_i(\omega)$ comprises both, the transmission line as well as the subscribers' input impedances $Z$. Please note, transmit and receive circuit are assumed to have infinite input impedance and hence both do not influence the transfer function. Moreover, noise sources are turned off when the transfer functions are measured and the receive amplifier's input is perfectly decoupled from its output.

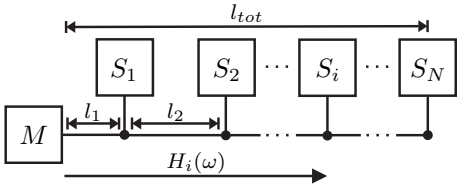


Fig. 2. Exemplary network topology in line structure with one master ($M$) and $N$ slaves ($S_i$). The transfer function from $M$ to $S_i$ is $H_i(\omega)$.

The scheme achieves bidirectional communication by applying time-division duplex [1]. In DL, the master communicates data to the slaves while in UL the opposite is true. According to our system model, the channel is symmetric, i.e.

$$H_i(\omega) = \frac{U_i(\omega)}{I_0(\omega)} = \frac{U_0(\omega)}{I_i(\omega)} \quad i = 1, \ldots, N \tag{2}$$

holds and hence $H_i(\omega)$ is independent in DL and UL.

Throughout this paper, we assume DMT transmission with $M$ carriers. When data transmission at DC ($k = 0$) is neglected, the discrete time-domain signal $s_{T,i}(n)$ of a single DMT symbol is [2]

$$s_{T,i}(n) = \sqrt{\frac{2}{M}} \sum_{k=1}^{M-1} a_{k,i}^R \cos\left(\frac{\pi}{M} nk\right) - a_{k,i}^I \sin\left(\frac{\pi}{M} nk\right) \tag{3}$$

while carrier $k$ of subscriber $i$ is modulated by the complex symbol $a_{k,i} = a_{k,i}^R + j a_{k,i}^I$. We further assume that $a_{k,i}^R$ and $a_{k,i}^I$ are uncorrelated, have zero mean, and that symbols $a_{k,i}$ of different subcarriers are uncorrelated as well. Additionally, the mean power of $a_{k,i}$ is normalized, i.e. $E[|a_{k,i}|^2] = 1$ holds. In this case, it can be shown that

$$S_{T,i}(\omega) = \frac{1}{4M^2} \sum_{k=1}^{M-1} c_{k,i} \left[\eta\left(\omega - \frac{\pi}{M}k\right) + \eta\left(\omega + \frac{\pi}{M}k\right)\right] \tag{4}$$

where $c_{k,i}$ and the short-hand notation $\eta(x)$ are defined as

$$c_{k,i} = \begin{cases} 1, & \text{when } a_{k,i} \neq 0 \\ 0, & \text{when } a_{k,i} = 0 \end{cases} \qquad \eta(x) = \frac{\sin^2(Mx)}{\sin^2(x/2)}.$$

In DMT transmission, DAC and ADC distortion namely $N_D$ and $N_A$ originate from two noise sources, respectively. On one hand, there is quantization noise which arises from the mapping of analog to discrete signal values and on the other hand there is clipping noise which results from amplitude limitation (clipping) of the DMT signal. The power of both noise sources behaves inversely to each other. In case amplitude limitation is high, clipping noise power will be low while quantization noise power is high and vice versa. Consequently, an optimum can be found where both noise sources contribute moderate distortion power. The analysis of the SNR due to clipping and quantization as well as its optimization has thoroughly been done in literature [7], [8]. Optimization yields maximum quantization SNR $\gamma_q$ at an optimal clipping ratio $\kappa_0 = A/\sigma$ with $A$ being the amplitude limitation and $\sigma$ being the signal power impinging on the converter. Table I gives an overview of $\gamma_q$, and $\kappa_0$ as a function of the resolution $b = \log_2 S$ bit of a converter with $S$ quantization steps. The provided results are valid when the amplitude of the DMT signal is Gaussian distributed and hold for both, DAC as well as ADC.

TABLE I. MAXIMUM $\gamma_q$ AND OPTIMAL $\kappa_0$ AS A FUNCTION OF $b$.

| $b$ [bit] | 4 | 6 | 8 | 10 | 12 |
|---|---|---|---|---|---|
| $\kappa_0$ | 2.6 | 3.3 | 4.0 | 4.5 | 5.0 |
| $\gamma_q$ [dB] | 19.7 | 29.9 | 40.6 | 51.6 | 62.7 |

## III. NOISE ANALYSIS

In the following, we compute the overall SNR which can be achieved between two subscribers in DL as well as in UL by considering the noise sources of the equivalent circuit.

### A. Downlink

In DL, we examine a connection between master ($\alpha_0$, $\beta_0$) and slave $i$ ($\alpha_i$, $\beta_i$). In this case, the PSD of the signal part at ADC output of Slave $i$ is

$$S_{R,i}(\omega) = \alpha_0 \beta_i \left|H_i(\omega)\right|^2 S_{T,0}(\omega) \tag{5}$$

where we made use of the Wiener-Khinchin theorem [9]. The PSD of the noise part at ADC output of Slave $i$ results in

$$N_{R,i}(\omega) = \alpha_0\beta_i \left|H_i(\omega)\right|^2 (N_D + N_{T0}) + \beta_i N_{R0} + N_A. \quad (6)$$

We assume that the ADC works in its optimal operating point $\kappa_0$. Consequently, amplification $\beta_i$ is adjusted such that $\kappa_0 = {}^{A}/_{\sigma_{R,i}}$ is fulfilled where $\sigma^2_{R,i}$ denotes the mean power of the signal part seen by ADC which is given by

$$\sigma^2_{R,i} = \alpha_0\beta_i \int_{-\pi}^{\pi} \left|H_i(\omega)\right|^2 S_{T,0}(\omega) \frac{\mathrm{d}\omega}{2\pi}. \quad (7)$$

With $\gamma_q$ and (7), we can readily compute $N_A$ to

$$N_A = \frac{\sigma^2_{R,i}}{\gamma_q} = \frac{\alpha_0\beta_i}{\gamma_q} \int_{-\pi}^{\pi} \left|H_i(\omega)\right|^2 S_{T,0}(\omega) \frac{\mathrm{d}\omega}{2\pi}. \quad (8)$$

In order to compute the DL SNR $\gamma_{i,D}(\omega)$ seen by slave $i$ on *every* carrier, we set $S_{T,0}(\omega) = 1$ which is the same than modulating all subcarriers or $c_{k,0} = 1\ \forall k$, respectively. Then,

$$\begin{aligned}\gamma_{i,D}(\omega)^{-1} = \gamma_{qD}^{-1} + \gamma_t^{-1} + \gamma_r^{-1} \frac{1}{\alpha_0 \left|H_i(\omega)\right|^2} \\ + \gamma_{qA}^{-1} \frac{\int_{-\pi}^{\pi} \left|H_i(\omega)\right|^2 \frac{\mathrm{d}\omega}{2\pi}}{\left|H_i(\omega)\right|^2}\end{aligned} \quad (9)$$

holds where we abbreviated the SNR of DAC, transmit and receive amplifier as well as ADC by $\gamma_{qD} = {}^{1}/_{N_D}$, $\gamma_t = {}^{1}/_{N_{T0}}$, $\gamma_r = {}^{1}/_{N_{R0}}$, and $\gamma_{qA} = {}^{1}/_{N_A}$, respectively.

Considering (9), the following observations can be made:

(i) Since (9) adds up the reciprocal values of the individual effective SNRs, it is dominated by the lowest effective SNR value(s).
(ii) Amplification $\alpha_0$ should be chosen has high as possible to reduce degradation on $\gamma_{i,D}(\omega)$ because of the effective receiver SNR which suffers from low channel gain.
(iii) Both, the contribution of $\gamma_r$ and $\gamma_{qA}$ depend on $H_i(\omega)$. Consequently, zeros in transfer function yield a low SNR.

Additionally, it is worth noting that $S_{T,0}(\omega)$ can equalize $\gamma_{i,D}(\omega)$ when the assumption of equal power for every carrier is relaxed. Carriers suffering from a deep fade can get more power than other carriers. However, this has to be done with respect to a power constraint which means that the power of a carrier can only be increased when a further carrier lowers its power. As we consider a multiuser scenario where carriers are allocated to different slaves this kind of optimization has to be done with respect to all slaves $i$ and their individual transfer functions to guarantee fairness among the slaves.

### B. Uplink

In UL, the master ($\alpha_0$,$\beta_0$) receive signal is a superposition of all slave signals. To avoid interference between slaves, each slave ($\alpha_i$,$\beta_i$) modulates exclusively its distinct carriers which have been allocated by the master before. Hence, the PSD of the signal part at the ADC of the master is given by

$$S_{R,0}(\omega) = \beta_0 \sum_{\lambda=1}^{N} \alpha_\lambda \left|H_\lambda(\omega)\right|^2 S_{T,\lambda}(\omega). \quad (10)$$

In contrast, the PSD of the noise part at the master ADC is

$$N_{R,0}(\omega) = \beta_0(N_D + N_{T0}) \sum_{\lambda=1}^{N} \alpha_\lambda \left|H_\lambda(\omega)\right|^2 + \beta_0 N_{R0} + N_A \quad (11)$$

Like in DL, the master ADC works in its optimal operating point $\kappa_0$. Therefore, $\beta_0$ is chosen such that $\kappa_0 = {}^{A}/_{\sigma_{R,0}}$ holds, and hence $N_A$ is given by

$$N_A = \frac{\sigma^2_{R,0}}{\gamma_q} = \frac{\beta_0}{\gamma_q} \int_{-\pi}^{\pi} \sum_{\lambda=1}^{N} \alpha_\lambda \left|H_\lambda(\omega)\right|^2 S_{T,\lambda}(\omega) \frac{\mathrm{d}\omega}{2\pi}. \quad (12)$$

As can be seen from (10) - (12), the UL SNR at the master receiver clearly depends on the specific carrier allocation. In order to get universal results, we analyze a scenario where one slave $i$ occupies all carriers, i.e. $S_{T,i}(\omega) = 1$ and all remaining slaves do not send any data. However, all slaves still emit wide-band noise $N_D$ and $N_{T0}$. Please note, this is an artificial scenario since $N_D$ is only present when data is sent. However, noise contributions are the same than in a multiuser UL scenario, except the ADC noise term which yields a specific solution for slave $i$ in this case. Thus, with (10) - (12) and $S_{T,i}(\omega) = 1$ we get

$$\begin{aligned}\gamma_{i,U}(\omega)^{-1} = \left(\gamma_{qD}^{-1} + \gamma_t^{-1}\right) \frac{\sum_{\lambda=1}^{N} \alpha_\lambda \left|H_\lambda(\omega)\right|^2}{\alpha_i \left|H_i(\omega)\right|^2} \\ + \gamma_r^{-1} \frac{1}{\alpha_i \left|H_i(\omega)\right|^2} + \gamma_{qA}^{-1} \frac{\int_{-\pi}^{\pi} \left|H_i(\omega)\right|^2 \frac{\mathrm{d}\omega}{2\pi}}{\left|H_i(\omega)\right|^2}\end{aligned} \quad (13)$$

which is the inverse of the overall UL SNR of slave $i$ at the master. When comparing the DL and UL SNR in (9) and (13), it is obvious that both lead similar results except a noise funneling term[1]

$$a_i = \frac{\sum_{\lambda=1}^{N} \alpha_\lambda \left|H_\lambda(\omega)\right|^2}{\alpha_i \left|H_i(\omega)\right|^2} \quad (14)$$

which leads to an enhancement of DAC and transmit amplifier noise. Minimization of $a_i$ is subject of the following section.

## IV. Optimization

### A. Minimization of noise funneling

In this section, we minimize[2] the noise funneling term $a_i$ by choosing appropriate $\alpha_i$. Considering slave $i$ for example, a large $\alpha_i$ clearly minimizes $a_i$. However, another slave $j$ ($j \neq i$) would suffer a stronger $a_j$ then. Thus, fairness between slaves is of particular importance and hence we present a joint minimization of $a_i$. In particular, the average noise funneling

$$\min_{\{\alpha_1,\ldots,\alpha_N\}} \sum_{i=1}^{N} a_i = \min_{\{\alpha_1,\ldots,\alpha_N\}} \sum_{i=1}^{N} \sum_{j=1}^{N} \frac{\alpha_j h_j}{\alpha_i h_i} \quad (15)$$

is minimized with respect to $(\alpha_1, \ldots, \alpha_N)$ where $h_i$ denotes the average channel gain which is

$$h_i = \int_{-\pi}^{\pi} \left|H_i(\omega)\right|^2 \frac{\mathrm{d}\omega}{2\pi}. \quad (16)$$

[1] Besides, $\gamma_r^{-1}$ in UL is scaled by ${}^{1}/_{\alpha_i}$ instead of ${}^{1}/_{\alpha_0}$ in DL, because in UL every slave transmits with its particular transmit amplification.

[2] Since (13) gives the reciprocal value of the UL SNR, maximum SNR is achieved for minimum $a_i$.

For solving (15), it is adequate to introduce

$$r_i = \frac{\alpha_{i+1} h_{i+1}}{\alpha_1 h_1} \quad i = 1 \ldots N-1 \tag{17}$$

and by an appropriate reordering, (15) can be rewritten as

$$f(r_1, \ldots, r_{N-1}) = N + \sum_{i=1}^{N-1} \left( r_i + \frac{1}{r_i} \right) + \sum_{i=1}^{N-1} \sum_{\substack{j=1 \\ j \neq i}}^{N-1} \frac{r_j}{r_i}. \tag{18}$$

The first derivative of (18) with respect to all $r_j$ must be zero for an optimum. Thus,

$$\frac{\partial f(r_1, \ldots, r_{N-1})}{\partial r_j} = 1 - \frac{1}{r_j^2} - \sum_{\substack{i=1 \\ i \neq j}}^{N-1} \frac{r_i}{r_j^2} + \sum_{\substack{i=1 \\ i \neq j}}^{N-1} \frac{1}{r_i} \tag{19}$$

holds and it can be seen that all partial derivatives vanish when $r_i = 1$ for $i = 1, \ldots, N-1$. In order to verify the kind of the optimum, the determinant of the Hessian matrix needs to be computed [10] which is omitted here due to space constraints. As a result, $r_i = 1 \ \forall i$ yields a minimum of (18) for $N > 1$. Recalling the definition of $r_i$, we see that all $a_i$ are jointly minimized when

$$\alpha_i = \alpha_i^{opt} = \frac{K}{h_i} \quad i = 1, \ldots, N \tag{20}$$

with $K > 0$ being any positive real constant. Furthermore, $a_i = N \quad \forall i$ holds when $\alpha_i = \alpha_i^{opt}$, i.e. every slave suffers the same average noise funneling.

It is worth noting that the average effective receiver UL SNR in (13) which is $\gamma_r \alpha_i h_i$ leads also the same value for all slaves when $\alpha_i = \alpha_i^{opt}$. This is because $\alpha_i^{opt}$ compensates for the near-far effect.

Please note, minimization is done here with respect to the average transmit amplification which compensates for the average channel gain but does not exploit the frequency-selective SNR. For that reason, the master allocates carriers to the slaves according to their individual SNR during initialization. The carriers may be distributed such that the overall data rate (sum-rate) is maximized by using the water filling algorithm [11]. In this case, there is no fairness since slaves with bad channel quality may get no carrier. Therefore, enhanced water filling algorithms [12] are applicable which optimize sum-rate with fairness consideration.

### *B. Optimization of DAC operating point*

In the following, we take a closer look to the DAC and its operating point in UL where usually only a small portion of the available subcarriers is modulated by each slave.

Fig. 3 shows a more detailed view of the transmit circuit shown in Fig. 1. Beside the noise sources $N_D$, $N_{T0}$, the transmit amplifier ($\sqrt{\widetilde{\alpha}_i}$), and the signal source $S_{T,i}(\omega)$ a clipping device which saturates the input signal at $\pm A$ as well as an amplification $\sqrt{\mu_i}$ were additionally added. Amplification $\sqrt{\mu_i}$ can be implemented in digital domain in advance of the DAC which is assumed to work in its optimal operating point. Consequently, $\mu_i$ is chosen such that the input power $\sigma_C^2$ to the clipping device fulfills

$$\kappa_0 = \frac{A}{\sigma_C}. \tag{21}$$

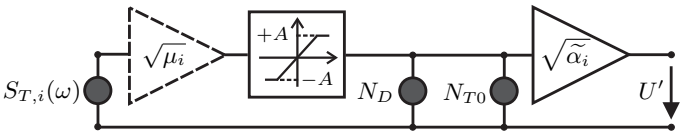


Fig. 3. Detailed block diagram of the enhanced transmit circuit.

Integrating (4) yields to the average signal power in UL

$$\sigma_T^2 = \frac{M_A}{M} = L \tag{22}$$

where $M_A$ out of $M$ carriers are modulated and $L$ denotes the loading ratio. In order to simplify notation, $L$ is assumed to be independent on slave index $i$. Combining (21), (22) with $\sigma_C^2 = \mu_i \sigma_T^2$, it can be easily shown that

$$\mu_i = \frac{1}{L} \left( \frac{A}{\kappa_0} \right)^2. \tag{23}$$

In order to keep the output power of the transmit circuit normalized, transmit amplification changes to $\widetilde{\alpha}_i = {}^{\alpha_i}/_{\mu_i}$.

$\mu_i$ according to (23) keeps $\sigma_C^2$ constant although less carriers are modulated. Consequently, the power per carrier is enhanced by $L^{-1}$, and the SNR of DAC and transmit amplifier increases because $N_D$ and $N_{T0}$ are fixed. In particular,

$$\gamma_{qD} = \frac{\gamma_q}{L} \quad \gamma_t = \frac{1}{L N_{T0}} \tag{24}$$

holds. Please note, the derivations on $\gamma_{qD}$ are only valid when the DMT signal amplitude is Gaussian distributed and when both clipping and quantization noise are frequency-flat. However, for a small $M_A$ the amplitude is no longer Gaussian distributed. Moreover, clipping noise as well as quantization noise get colored for small $L$. Therefore, we simulate $\gamma_{qD}$ as a function of $\kappa$ and $L$ for various $M$. The results for a DAC resolution of 10 bit are shown in Fig. 4. For $L = 1$, we can see that $\kappa_0 = 4.5$ of Tab. I clearly maximizes $\gamma_{qD}$. Left hand side of $\kappa_0$ clipping noise dominates whereas on the right hand side quantization noise is the major noise source.

Considering $M = 1024$, $\kappa_0$ slightly increases for small $L$. This is because of clipping noise which is rather concentrated inside transmission band than out-of-band. Consequently, active carriers face an enhanced clipping noise which is lowered by an increasing $\kappa_0$ for an optimal clipping and quantization noise trade-off. Maximum $\gamma_{qD}$ behaves like indicated by (24) and it is enhanced by 15 dB when comparing $L = 0.03125$ with $L = 1$. However, if we consider $M = 128$ optimum $\kappa$ depends strongly on $L$. This is because the amplitude distribution is no longer Gaussian since for $L = 0.0625$ only $M_A = 8$ carriers are modulated. For the same reason, SNR gains are higher than indicated by (24). Moreover, periodic fluctuations in $\gamma_{qD}$ for $L = 0.03125$ are due to colored quantization noise.

Optimization methods of IV-A and IV-B can be applied independently. While method IV-A requires a channel estimation algorithm for computing $h_i$, method IV-B needs knowledge of $L$. In scenarios where the slaves changes their data rate instantaneously $L$, $\mu$, and $\widetilde{\alpha}_i$ change rapidly. In case $\widetilde{\alpha}_i$ can not be adjusted that fast $L$ can also be chosen to a fixed maximum value $L_{max}$. In case $L_{max} < 1$, SNR performance still enhances.

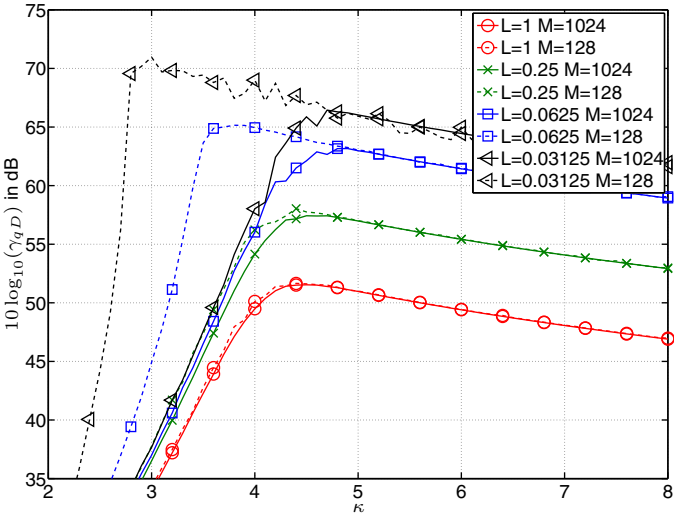


Fig. 4. SNR of the DAC due to clipping and quantization as a function of $\kappa$ and $L$. The converter features $b = 10$ bit and the DMT scheme has $M = 128$ and $M = 1024$ carriers, respectively.

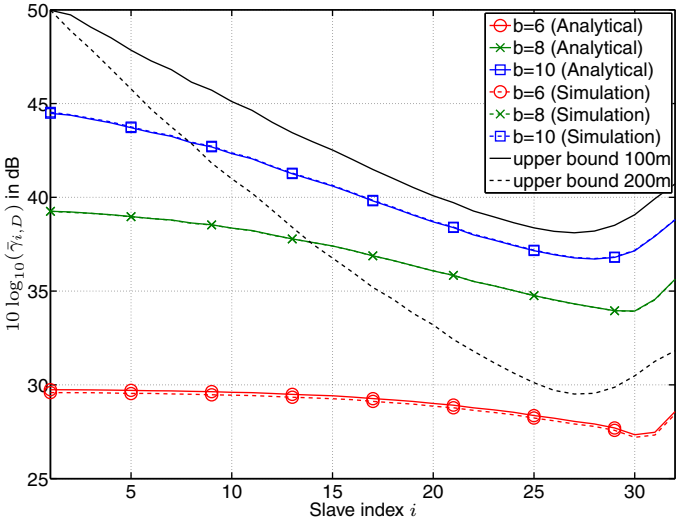


Fig. 5. SNR in downlink as a function of slave index $i$ and various DAC resolutions of $b$ bit while the ADC features 10 bit. Beside analytical and simulation results, the upper bounds for $l_{tot} = 100$ m and 200 m are shown.

## V. Simulation Results

In this section, we provide selected results that illustrate the SNR conditions in our multiuser scheme. The system we analyze has $N = 32$ slaves and $M = 1024$ carriers in total. As the results depend on the subscribers' transfer functions, we simulated $H_i(\omega)$ in the network topology shown in Fig. 2. We generated 100 different network setups by choosing the distances $l_i$ between the slaves randomly while maintaining $l_{tot} = 100$ m unless otherwise noted. The cable parameters were set to typical values for a non-shielded two-wire cable

$$L' = 0.5\frac{\mu H}{m} \quad R' = 0.3\frac{\Omega}{m} \quad C' = 0.1\frac{nF}{m} \quad G' = 80\frac{\mu S}{m}$$

and the skin effect was neglected. Input impedance $Z$ was selected to the equivalent of a parallel circuit with elements $R = 10\ k\Omega$ and $C = 0.1nF$, respectively. Moreover, we set

$$N_{T0} = N_{R0} = 10^{-9}\ \frac{V^2}{rad} \quad S_{T,i}(\omega) = 10^{-4}\ \frac{V^2}{rad}$$

for simulation where the latter holds when all carriers are modulated. The results shown in the following give $\bar{\gamma}_{i,D}$ and $\bar{\gamma}_{i,U}$ which is an average SNR of $\gamma_{i,D}(\omega)$ and $\gamma_{i,U}(\omega)$ with respect to frequency and network realization, respectively.

Fig. 5 shows $\bar{\gamma}_{i,D}$ in DL as a function of slave index $i$. Both, analytical and simulation results are plotted for various DAC resolutions of $b$ bit while the ADC features 10 bit. The master transmit amplification $\alpha_0$ is chosen such that it compensates for $h_1$.

First of all, it can be seen that analytical and simulated results match perfectly for all considered scenarios. Moreover, it is obvious that with increasing DAC resolution the transmission quality improves considerably. However, when comparing $b = 8$ with $b = 10$ improvements in $\bar{\gamma}_{i,D}$ are marginal for a high $i$ because system performance is mainly dominated by $N_{R0}$ and $N_{T0}$. As a result, SNR approaches the upper bound for $b = 10$ and $l_{tot} = 100$ m which denotes the performance with transmit and receive amplifier noise only. Additionally, $\bar{\gamma}_{i,D}$ tends to degrade for increasing $i$ because of the near-far effect in DL resulting in a maximum loss of 8 dB for $b = 10$. The reason for that is shown in (9) where $\gamma_r$ is weighted by the channel attenuation which tends to increase with $i$. For comparison, the upper bound for $l_{tot} = 200$ m is also plotted. Here we can clearly see a severe degradation in $\bar{\gamma}_{i,D}$ for slaves with high $i$ which suffer from low signal power because of their strong channel attenuation. In this case, the upper bound is mainly dominated by receive amplifier noise since the ADC with $b = 10$ limits the SNR to 51.6 dB according to Tab.I.

Fig. 6 shows $\bar{\gamma}_{i,U}$ in UL as a function of slave index $i$ for various DAC resolutions of $b$ bit. The ADC resolution is fixed at 10 bit. Transmit amplification is adapted either to each slave $\alpha_i = \alpha_i^{opt}$ or to slave 1, i.e. $\alpha_i = \alpha_1^{opt}$. For reference purposes, upper bounds are plotted which give $\bar{\gamma}_{i,U}$ if both DAC and ADC feature infinitely high resolution. For now, we set $\mu = {}^{A}/_{\kappa_0}$, hence adaption with respect to $L$ is omitted.

Clearly, $\bar{\gamma}_i$ enhances with increasing $b$. For $b = 10$ the SNR approaches the upper bound and consequently a further increase $b > 10$ yields only marginal SNR gains. Considering $\alpha = \alpha^{opt}$, it can be observed that $\bar{\gamma}_{i,U}$ gets almost independent of $i$ and fairness among the slaves is achieved. Clearly, due to this optimization closer slaves suffer more noise and have less SNR compared to $\alpha \neq \alpha^{opt}$. However, when considering the area between the dash-dotted and solid line which gives the accumulated SNR of all slaves, it can clearly be observed that $\alpha = \alpha^{opt}$ yields a gain in overall SNR. Please note, when comparing $\bar{\gamma}_{i,U}$ with $\bar{\gamma}_{i,D}$ in Fig. 5 the UL SNR is still lower than in DL because of $\mu$ is not adapted to $L$.

Fig. 7 shows both, analytical and simulation results of $\bar{\gamma}_{i,U}$ with $\alpha_i = \alpha_i^{opt}$. Now, the DAC operating point of each slave is adapted to $L$. Additionally, we assume that all slaves share bandwidth equally, i.e. every slave transmits on $M_A = 32$ out of $M = 1024$ carriers. Consequently, $L_{max} = 0.03125$ holds.

First of all, analytical and simulation results are in perfect agreement. Both clearly show that the lower $L$ the higher the SNR gain is because noise contributions of the transmitter and

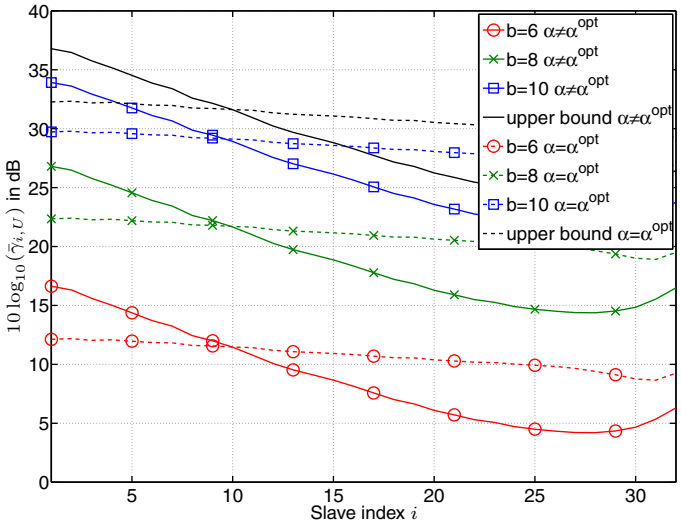


Fig. 6. SNR in uplink as a function of slave index $i$ and various DAC resolutions of $b$ bit. The ADC features 10 bit and transmit amplification is either adapted to the channel ($\alpha = \alpha^{opt}$) or kept constant ($\alpha \neq \alpha^{opt}$).

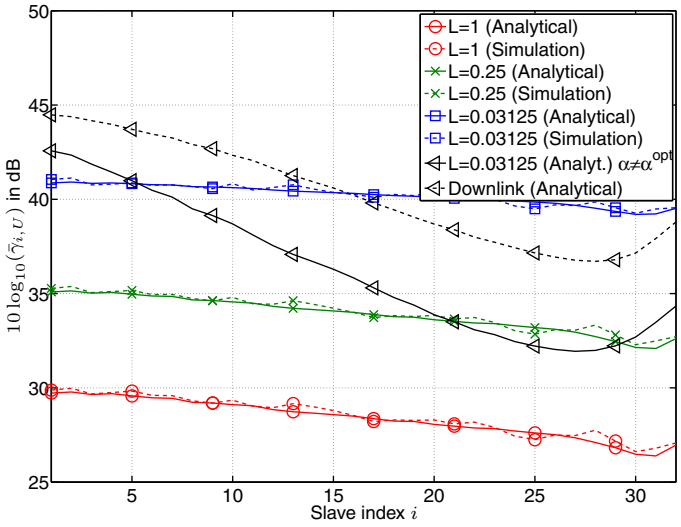


Fig. 7. SNR performance in uplink with $\alpha_i = \alpha_i^{opt}$. The DAC operating point is adapted to various $L$ values and DAC as well as ADC feature $b = 10$ bit. Simulation and analytical results are compared.

DAC are significantly reduced. The average SNR gain accounts to more than 10 dB when $L = 0.03125$ is compared to $L = 1$. In contrast to the results of Fig. 6, this substantial gain can not be achieved because of the upper bound which limited performance before and which is now shifted to higher SNR regions. Fig. 7 also shows $\bar{\gamma}_{i,U}$ in the case that $\alpha \neq \alpha^{opt}$. Here we clearly see that the adaption of $\alpha_i$ yields beside fairness also a significant gain in the SNR performance of the whole system. The gains achieved are even greater than in the case that the DAC operating point is not adapted to $L$. Comparing SNR in DL and UL, the system performance in terms of the overall SNR is equal while in contrast to UL, the DL provides less user fairness. However, fairness in DL can be easily achieved with an adequate power loading where carriers belonging to slaves with high $i$ get more power while those with low $i$ reduce their power simultaneously. As a result, SNR performance in UL is comparable to DL when both optimization techniques are applied.

## VI. Conclusion

We have presented a detailed SNR analysis of a bidirectional multiuser fieldbus communication scheme with DMT transmission where all major noise sources have been considered. We have performed a theoretical analysis of the scheme and derived analytical expressions of the achievable SNR in both down- and uplink. It has been shown that the SNR in uplink suffers a strong noise funneling which limits system performance. Therefore, we have derived two optimization techniques which yield a minimization of noise funneling and a maximization of user fairness by compensating for the near-far effect. Finally, analytical SNR values were shown to be in very good agreement with simulated results and both illustrated that the presented optimization techniques yield significant SNR gains so that comparable SNR performance in down- and uplink can be achieved.

## Acknowledgment

This work was partly funded by the German Federal Ministry of Economics and Technology (BMWi 16IN0672).

## References

[1] T. Handte, M. Breuninger, H. Hagmeyer, and J. Speidel, "Physical Layer of a Novel Broadband Low-Level Fieldbus with Discrete Multitone," in *9th IEEE Int. Workshop on Factory Commun. Syst.*, May 2012, pp. 173–176.

[2] R. Schur, S. Pfletschinger, and J. Speidel, "DMT Modulation," in *Wiley Encyclopedia of Telecommunications*, J. G. Proakis, Ed. Wiley and Sons, 2003, vol. 2, pp. 736–748.

[3] M. Breuninger and J. Speidel, "Performance of Combined Error Correction and Error Detection for very Short Block Length Codes," in *IEEE Int. Symp on Ind. Electron.*, May 2012, pp. 1209–1213.

[4] K.-P. Kirchner, A. Fink, M. Voss, and H. Beikirch, "Packet-Based Time-Critical Medium Access for a Process-Oriented Deterministic Bus System," in *17th IEEE Int. Conf. on Emerging Technol. and Factory Automat.*, Sept. 2012, pp. 1–4.

[5] K.-P. Kircher and C. Huschka, "Identifying Nodes in a Master-Slave-Fieldbus," in *7th IEEE Int. Conf. on Intell. Data Acquisition and Advanced Computing Syst.*, Sept. 2013.

[6] T. Rudloff, A. Fink, M. Voss, M. Flügge, K. P. Kirchner, T. Heimbold, and H. Beikirch, "Emulation of a digital Process-Oriented Real-Time Communication Circuit," in *11th IFAC/IEEE Int. Conf. on Programmable Devices and Embedded Syst.*, May 2012, pp. 286–290.

[7] D. Mestdagh, P. Spruyt, and B. Biran, "Effect of amplitude clipping in DMT-ADSL transceivers," *Electron. Lett.*, vol. 29, no. 15, pp. 1354–1355, Jul. 1993.

[8] D. Dardari, "Joint Clip and Quantization Effects Characterization in OFDM Receivers," *IEEE Trans. on Circuits and Syst. I: Reg. Papers*, vol. 53, no. 8, pp. 1741–1748, Aug. 2006.

[9] A. Papoulis and S. Unnikrishna Pillai, *Probability, Random Variables, and Stochastic Processes*, 4th ed. Boston: McGraw-Hill, 2002.

[10] A. Antoniou and W.-S. Lu, *Practical Optimization: Algorithms and Engineering Applications*, 1st ed. New York: Springer, 2007.

[11] G. Münz, S. Pfletschinger, and J. Speidel, "An Efficient Waterfilling Algorithm for Multiple Access OFDM," in *IEEE Global Telecommun. Conference*, vol. 1, Nov. 2002, pp. 681–685.

[12] L. Gao and S. Cui, "Efficient Subcarrier, Power, and Rate Allocation with Fairness Consideration for OFDMA Uplink," *IEEE Trans. on Wireless Commun.*, vol. 7, no. 5, pp. 1507–1511, May 2008.

[13] K. Jacobsen, "Discrete Multi-Tone Modulation for High-Speed Upstream Communications on HFC Networks," in *31th Asilomar Conf. on Signals, Syst., and Computers*, vol. 1, Nov. 1997, pp. 585–589.